Journal of Catalysis 271 (2010) 315–324

Contents lists available at ScienceDirect

Journal of Catalysis

journal homepage: www.elsevier.com/locate/jcat

Promoting effect of transition metal-doped Co–B alloy catalysts for hydrogen production by hydrolysis of alkaline $NaBH_4$ solution

N. Patel *, R. Fernandes, A. Miotello

Dipartimento di Fisica, Università degli Studi di Trento, I-38100 Povo, Trento, Italy

ARTICLE INFO

Article history:
Received 17 December 2009
Revised 8 February 2010
Accepted 9 February 2010
Available online 19 March 2010

Keywords:
H_2 generation
Hydrolysis
Sodium borohydride
Doped Co–B catalyst
Surface area

ABSTRACT

A systematic and comparative study is conducted on Co–B-based ternary alloy catalysts for H_2 generation by hydrolysis of $NaBH_4$. Various transition metals, namely Ni, Fe, Cu, Cr, Mo, and W, were added to Co–B catalyst by chemical reduction of the corresponding metal salts. All the transition metals in the Co–B compounds behave in a dissimilar manner while influencing the catalytic activity. Cr, W, Mo, and Cu impose significant promoting effects on the Co–B catalyst by increasing the H_2 generation rate by 3–4 times when compared to the undoped catalyst. On the contrary, Ni and Fe are only able to create a marginal increment in the catalytic performance of the Co–B catalyst. The metal/(Co + metal) molar ratio was varied in the catalyst in order to study the effect of metal doping on surface morphology, electronic interaction, and catalytic efficiency of the alloy catalyst. This systematic variation also contributed to clarify the role of each dopant metal in the electron exchange mechanism involved in $NaBH_4$ hydrolysis. The promoting effects of the dopant metals are mainly discussed in terms of large active surface area, ability to act as Lewis acid sites for better absorption of OH^- group, electronic interaction with Co active metal, and amorphous nature of the alloy catalyst.

1. Introduction

Commercialization of fuel cell-based portable devices is hindered by the lack of an efficient and safe medium for hydrogen storage and generation. Chemical hydrides like sodium borohydride ($NaBH_4$) have attracted worldwide interest as a source to supply pure hydrogen to fuel cells at room temperature, because it is stable in alkaline solution, non-flammable, non-toxic in nature, and with hydrogen storage capability of 10.8 wt.% [1]. Furthermore, hydrogen is generated by a water-based hydrolysis reaction of $NaBH_4$ with the advantage of producing half of the hydrogen from the water solvent [2]. However, a catalyst is required to accelerate this hydrolysis reaction in a controllable manner. Therefore, the catalyst is the key factor that affects the H_2 generation rate by hydrolysis of $NaBH_4$. Solid-state catalysts such as precious metals (generally functionalized with support) [3–5] or transition metals [6,7] and their salts are found to be very efficient in accelerating the hydrolysis reaction in a controllable manner.

Amorphous cobalt–boride (Co–B) catalysts, prepared by reduction of metal salts with a reducing agent, have attracted great attention in catalysis owing to their unique properties such as isotropic structure, high concentration of coordinative unsaturated sites, relevant chemical stability, and low cost [8]. However, the exothermic nature of the reduction reaction involves high surface energy causing Co–B particles to agglomerate. This particle agglomeration lowers the effective surface area of the catalyst powder thus limiting its catalytic activity. In recent years, several routes have been adopted to improve the catalytic activity of the Co–B catalyst, mainly by increasing the surface area. This was accomplished by depositing Co–B on a support material having high specific surface area [9,10] or by using organic templates during the reduction reaction [11]: the final surface area of these catalyst powders is much higher than that of the "normal" Co–B powder. Nanoparticle-assembled Co–B catalysts films synthesized by pulsed laser deposition technique showed a performance similar to that of the noble metals because of the achieved high surface area [7,12].

Another efficient route to avoid agglomeration of Co–B particles is by introducing, between them, an atomic diffusion barrier in the form of transition metals like Cr, Mo, or W [13]. These promoter metals, mainly in form of oxides, are really efficient and even a small atomic concentration is able to significantly increase the surface area of the metal–borides catalyst powder [14] by avoiding agglomeration. In addition, they also contribute to the overall catalytic reaction by acting as acidic sites to improve the absorption of the reactant species on the surface [15]. The second metal also acts as an electron donor ligand, thus increasing the electron density on the active metal atoms which favors the reaction kinetics [16]. These combined effects, along with the simple preparation method, make such alloy catalysts very attractive. Our previous reports

* Corresponding author. Address: University of Trento, Department of Physics, Via Sommarive, 14, I-38050 Povo, Trento, Italy.
E-mail address: patel@science.unitn.it (N. Patel).

0021-9517/$ - see front matter © 2010 Elsevier Inc. All rights reserved.
doi:10.1016/j.jcat.2010.02.014

proved that the alloys exhibit superior catalytic activity in hydrogen production by hydrolysis of $NaBH_4$ [14,16–18]. There are available literatures [14–16] on transition metal-doped Co–B catalyst used for different reactions, but none of the published papers compares the effect of the different dopants for a single specified reaction. Thus, it is very important to make a comparative analysis on the promoting effects of different dopants in Co–B catalyst, for a single specified reaction, to gain insight into the involved mechanisms.

In the present work, we investigated the effect of various dopant transition metals (such as Ni, Fe, Cu, Cr, Mo, and W) in Co–B catalyst powder on hydrogen production by hydrolysis of $NaBH_4$. We discovered that these dopant metals behave in a specific manner to enhance the catalytic performance of the Co–B catalyst. On the basis of characterization results, the role of each metal species, in the electron exchange mechanisms involved in the $NaBH_4$ hydrolysis, is discussed.

2. Experimental

Ternary alloy catalysts in the form of Co–Ni–B, Co–Fe–B, Co–Cu–B, Co–W–B, Co–Cr–B, or Co–Mo–B powder were synthesized by mixing nickel chloride ($NiCl_2$), iron chloride ($FeCl_2$), copper nitrate ($Cu(NO_3)_2$), sodium tungstate dihydrate ($Na_2O_4W{\cdot}2H_2O$), chromium nitrate ($Cr(NO_3)_3$), or molybdenum chloride ($MoCl_2$) salts, respectively, in the cobalt chloride ($CoCl_2$) aqueous solution. Further, these different mixture solutions were reduced by the sodium borohydride ($NaBH_4$) under vigorous stirring. An excess amount of borohydride was used in order to completely reduce the metal cations. The black powder separated from the solution during reaction course was filtered and then extensively washed with distilled water and ethanol before drying at around 323 K under continuous N_2 flow. The metal to cobalt molar ratio (χ_M = M/(M + Co), where M = Ni, Fe, Cu, W, Cr or Mo) was adjusted in the final ternary alloy catalysts by varying the molar concentration of metal salts to cobalt salt in the aqueous solution. For comparison, we also prepared Co–B powder with same procedure by reducing only cobalt salt.

The surface morphology of all catalyst powders was studied by scanning electron microscope (SEM-FEG, JSM 7001F, JEOL) equipped with energy-dispersive spectroscopy analysis (EDS, INCA PentaFET-x3) to determine the composition of the samples. Structural characterization of the catalyst powders was performed by conventional X-ray diffraction (XRD) using the Cu K_α radiation (λ = 1.5414 Å) in Bragg–Brentano (θ–2θ) configuration. Surface electronic states and the related atomic composition of the catalysts were determined by using X-ray photoelectron spectroscopy (XPS). X-ray photoelectron spectra were acquired using a SCIENTA ESCA200 instrument equipped with a monochromatic Al K_α (1486.6 eV) X-Ray source and a hemispherical analyzer. No electrical charge compensation was required to perform XPS analysis. The BET surface area of the powder catalysts was determined by nitrogen absorption at 77 K (Micromeritics ASAP 2010) after degassing.

For catalytic activity measurements, an alkaline-stabilized solution of sodium borohydride (pH 13, 0.025 ± 0.001 M) (Rohm and Haas) was prepared by the addition of NaOH. The titer of reagent was independently measured through an iodometric method [19]. The generated hydrogen quantity was measured through a gas volumetric method in an appropriate reaction chamber with thermostatic bath which maintains constant temperature within accuracy of ±0.1 K. The chamber was equipped with a pressure sensor, stirrer system, catalyst insertion device, and also coupled with an electronic precision balance to accurately measure the weight of water displaced by the hydrogen produced during the reaction course. A detailed description of the measurement apparatus is reported in reference [20]. In all measurement runs, the catalyst was placed on the insertion device inside the reaction chamber and the system was sealed. Catalyst powder was added to 200 ml of the above solution, at 298 K, under continuous stirring. For comparison, the stoichiometric cumulative hydrogen production yield (%) versus time was plotted instead of the hydrogen volume (ml) versus time. The H_2 generation rate was measured at different solution temperatures to determine the activation energy involved in the catalytic hydrolysis reaction for all the catalysts.

To prove that metal cationic species, in Co–B catalyst, act as a Lewis acid site in the absorption of OH^- group during catalytic hydrolysis reaction, two types of hydride solution (0.025 M) were prepared, namely: (1) $NaBH_4$ solution stabilized with NaOH (0.025 M) (designated as solution A) and (2) $NaBH_4$ solution without NaOH (designated as solution B). Hydrogen generation rate was measured by hydrolysis of solutions A and B using all ternary alloy catalysts and Co–B catalyst powders.

3. Results and discussion

First of all, the effect of dopants concentration on the catalytic activity of Co–B catalyst was studied by synthesizing the alloy catalyst with different metal/(Co + metal) (χ_M) molar ratio. Fig. 1a–f presents the hydrogen generation yield, as function of time, measured by hydrolysis of alkaline $NaBH_4$ (0.025 M) solution using Co–Ni–B, Co–Fe–B, Co–Cu–B, Co–Cr–B, Co–Mo–B, and Co–W–B catalyst powders with different Ni, Fe, Cu, Cr, Mo, and W concentration, respectively. Inset of Fig. 1 presents the plot of R_{max} value (the maximum H_2 generation rate, for all the catalyst powders, which we established by a numerical procedure described elsewhere [12]) as a function of χ_M% (where M = Ni, Fe, Cu, Cr, Mo, and W). The H_2 generation rate increases with the increase in χ_M% and reaches the maximum with χ_{Ni} = 15%, χ_{Fe} = 35%, χ_{Cu} = 35%, χ_{Cr} = 4%, χ_{Mo} = 5%, and χ_W = 5%. With further increase in χ_M, the activity of the powder decreases (each measurement is repeated at least three times). The promoting effect of Cr, Mo, and W on catalytic activity is achieved at low concentration doping (4–5 molar%), and it is so evident that even a small amount of doping (~1 molar%) is able to double the activity of the Co–B catalyst. Much higher concentrations of Ni, Fe, and Cu have to be used in Co–B catalyst to attain a pronounced promoting effect in H_2 generation rate. No significant effect was observed on the catalytic activity of Co–B catalyst with low concentration (below 10 molar%) doping of these metals (Ni, Fe, and Cu).

Comparative analysis of the alloy catalysts powders was carried out with χ_M% values where R_{max} is highest (see inset of Fig. 1), for the hydrolysis of $NaBH_4$. Hydrogen generation yield was measured, as a function of time, during the hydrolysis of alkaline $NaBH_4$ (0.025 M) solution in presence of Co–B, Co–Ni–B (χ_{Ni} = 15%), Co–Fe–B (χ_{Fe} = 35%), Co–Cu–B (χ_{Cu} = 35%), Co–Cr–B (χ_{Cr} = 4%), Co–Mo–B (χ_{Mo} = 5%), and Co–W–B (χ_W = 5%) powder catalysts at 298 K (Fig. 2). The expected total amount of H_2 was measured irrespective of the type of catalyst used. The H_2 generation yield values, reported in Fig. 2, were perfectly fitted by using a single exponential function [17], as described by:

$$[H_2](t) = [H_2]_{max} \times (1 - e^{-k_1 t}) = 4[[BH_4^-]_0 \times (1 - e^{-k_1 t})] \quad (1)$$

where $[BH_4^-]_0$ is the initial molar concentration of $NaBH_4$ in the solution and k_1 is the overall rate constant of the first-order reaction. This indicates that hydrolysis reaction is first-order reaction with respect to $NaBH_4$. In the present case, a low hydride/catalyst ratio was used which means that the first-order kinetics involving diffusion of BH_4^- on the catalyst surface is the rate-limiting step during the hydrolysis reaction (see discussion reported in Ref. [17]). R_{max},

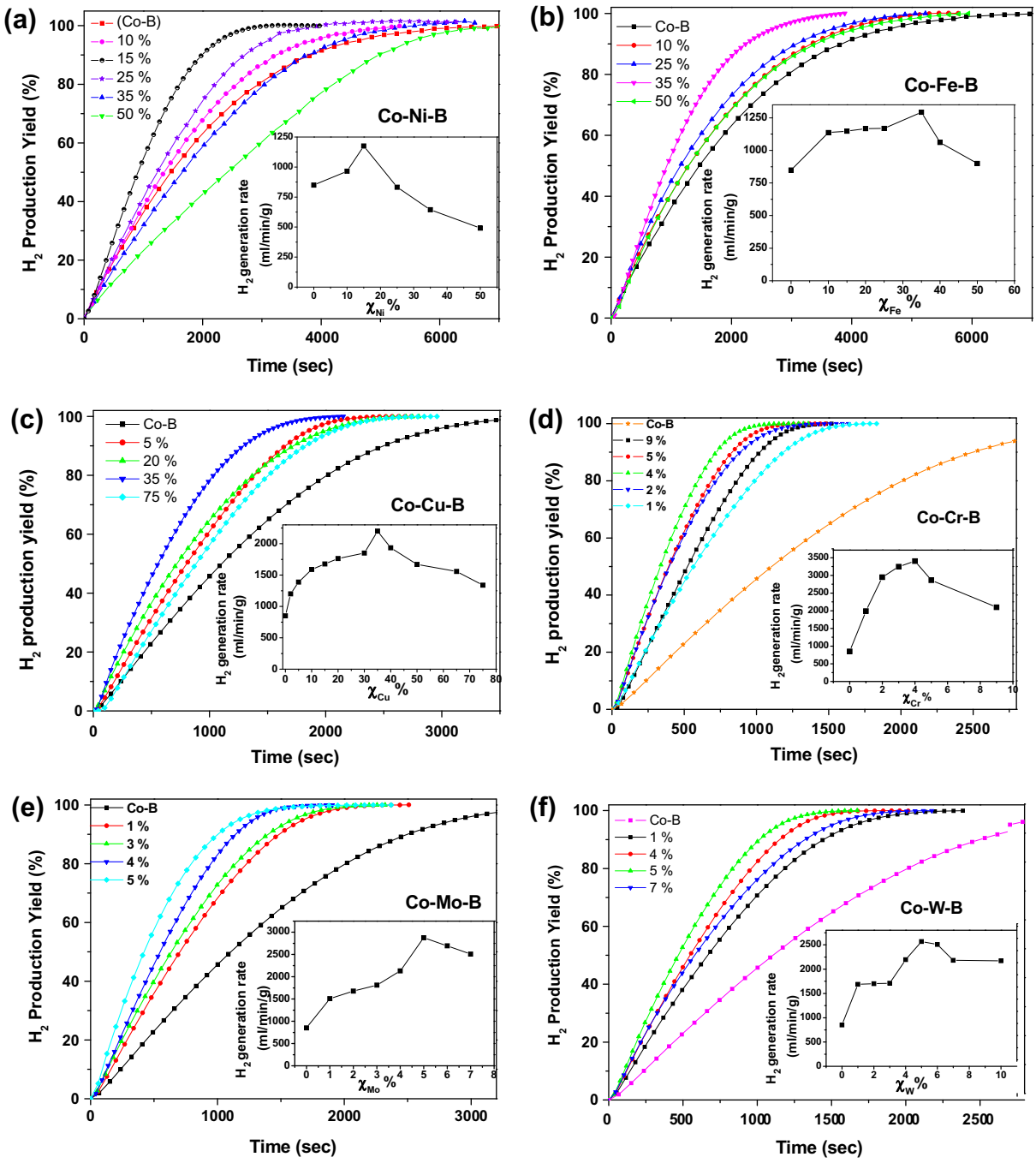

Fig. 1. Hydrogen generation yield as a function of reaction time obtained by hydrolysis of alkaline $NaBH_4$ (0.025 M) with (a) Co–Ni–B, (b) Co–Fe–B, (c) Co–Cu–B, (d) Co–Cr–B, (e) Co–Mo–B, and (f) Co–W–B with different χ_M values (where M = Ni, Fe, Cu, Cr, Mo, and W). Inset shows the maximum H_2 generation rate (R_{max}) as a function of χ_M.

for all the catalyst powders, are summarized in Table 1. We observe that these values decrease in the following order: Co–Cr–B > Co–Mo–B > Co–W–B > Co–Cu–B > Co–Fe–B > Co–Ni–B > Co–B. The measurements are repeated at least three times to verify the obtained results. The Co–Cr–B catalyst powder (~3400 ml/min/g), with χ_{Cr} = 4%, shows about four times higher H_2 generation rate when compared to that achieved with Co–B catalyst powder (~850 ml/min/g). The above results prove that doping Co–B powder with whichever of the transition metal (Cr, Mo, W, Cu, Fe, and Ni), with small or large concentration, enhances the catalytic efficiency of the catalyst.

Morphological, structural, and electronic changes, occurring in the Co–B powder with addition of the different transition metals, have been studied to understand the promoting role of each transition metal.

In Fig. 3, we present the SEM images of all the alloy powder catalysts. All samples show similar particle-like morphology with particles having spherical shape and size of a few nanometers. During catalyst preparation, the use of $NaBH_4$ as a reducing agent causes a fast reduction of Co ions that inhibits particle growth above a few nanometers. However, at higher SEM magnification, it is evident that these particles are mostly in agglomerated state in the case of Co–B, Co–Ni–B, and Co–Fe–B powders. On the contrary, a lower degree of agglomeration is observed with Co–Cu–B, Co–W–B, Co–Cr–B, and Co–Mo–B powders, and such a morphology is helpful to enhance the active surface area of catalysts (as discussed later

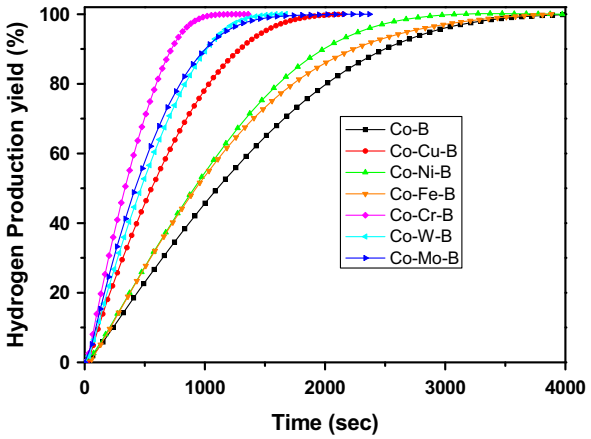

Fig. 2. Hydrogen generation yield as a function of reaction time obtained by hydrolysis of alkaline $NaBH_4$ (0.025 M) with Co–B, Co–Ni–B (χ_{Ni} = 15%), Co–Fe–B (χ_{Fe} = 35%), Co–Cu–B (χ_{Cu} = 35%), Co–Cr–B (χ_{Cr} = 4%), Co–Mo–B (χ_{Mo} = 5%), and Co–W–B (χ_{W} = 5%) powder catalysts at 298 K.

on the basis of BET measurement). XRD patterns (Fig. 4) of all the Co–B-based alloy powders show a broad peak at around $2\theta = 45°$, which is assigned to the amorphous state of Co–B alloy. Other broad peaks at around 35° and 43°, attributed to the presence of Cr_2O_3 and Cu metal, are also observed for Co–Cr–B and Co–Cu–B catalyst powders, respectively. Finally, the diffraction spectra indicate short-range order and long-range disorder, and both these features might contribute to enhance the catalytic activity [21].

XPS was used to gain insight into the electronic states and surface interaction between atoms in all catalyst compounds. Fig. 5a and b shows the XPS spectra of $Co_{2p3/2}$ and B_{1s} electronic levels, respectively, in all the catalyst powders. Two peaks appear, for all the catalyst compounds, corresponding to the $Co_{2p3/2}$ level at the binding energies (BE) in a range of 778.2–778.4 and 781.6–781.8 eV. This suggests that Co element exists in both elemental and oxidized states, respectively. The +2 state related to the peak of the oxidized cobalt is attributed to $Co(OH)_2$: this molecule would have been formed possibly during catalyst preparation [22] or when it was exposed to ambient atmosphere before transferring to the reaction chamber. This cobalt hydroxide ($Co(OH)_2$) does not cause major effects on catalytic activity, because it can be easily reduced by sodium borohydride in the course of the hydrolysis forming Co–B active phase. Liu and Li [23] showed experimentally that $Co(OH)_2$ intermediate acts as nuclei for the precipitation of Co–B active phase during the reaction with $NaBH_4$. There is no significant shift in the present Co BE peak when compared to the standard binding energy of metallic Co for all the catalyst powders, except for the Co–Ni–B catalyst. Two XPS peaks are also observed at BE values of 188.1–188.3 eV and 192.1–192.3 eV, which correspond to elemental and oxidized B_{1s} levels, respectively, for all catalyst powders [22]. A positive shift of around 1.0–1.2 eV is evident when comparing the BE of pure boron (187.1 eV) to that of boron in the catalyst. This shift indicates an electron transfer from alloying B to vacant d-orbital of metallic Co, which makes the B atom electron deficient and the Co atom electron enriched: this is true for all the catalyst powders [24]. The lack of shift in Co peak in compound catalyst is due to the heavy mass of the atom.

Fig. 6a–f presents the XPS spectra of Ni_{2p}, Fe_{2p}, Cu_{2p}, Cr_{2p}, Mo_{3d}, and W_{4f} electronic levels in Co–Ni–B, Co–Fe–B, Co–Cu–B, Co–Cr–B, Co–Mo–B, and Co–W–B, powders, respectively. The XPS result for each catalyst powder is separately discussed below:

1. *Co–Ni–B:* Two peaks appear in $Ni_{2p3/2}$ levels with binding energies of 852.6 and 856.3 eV (Fig. 6a), indicating that Ni metal exists in both the elemental and oxidized states, respectively. The oxide is mainly in the form of $Ni(OH)_2$ which would have been formed during the catalyst preparation reaction between $NaBH_4$ and metal salts, similarly to cobalt oxide. However, only a few amount of Ni is present in oxidized form (15 at.%), while most of it is in the form of metallic Ni (85 at.%). The BE of metallic Co in Co–Ni–B is 0.2 eV lower than that in the Co–B, whereas BE of metallic Ni in Co–Ni–B is also 0.2 eV lower than that in Ni–B [16]. This proves that in Co–Ni–B catalyst, there is an electronic enrichment on Co and Ni metals when compared with the Co–B and Ni–B catalysts: this is mainly attributed to the B-enrichment in Co–Ni–B catalyst as seen by the compositional analysis of XPS spectra (as reported in our previous work [16] and also reported by Li et al. [25]). These authors also performed theoretical calculations using DFT method to show that the increase in the B content on the surface would contribute more electrons to metallic Ni or Co in their corresponding amorphous alloys [25].
2. *Co–Fe–B:* The elemental Fe in Co–Fe–B catalyst is present in both metallic and oxidized state with binding energies of 707.1 and 712.7 eV, respectively (Fig. 6b). The oxidized Fe species on the catalyst surface is mostly in the form of Fe_2O_3 state (90 at.%) probably formed during the preparation. The metallic Fe (10 at.%) shows a positive shift of about 0.3 eV in its corresponding BE peak, which suggests electron transfer from Fe to Co atoms. However, no shift is observed in the BE of the Co peak probably because a few Fe atoms are present in metallic state to transfer electrons to Co atoms.
3. *Co–Cu–B:* For Cu, only a single peak corresponding to a metallic state is apparent at BE of 932.6 eV (Fig. 6c). This is consistent with XRD result which signals indeed the presence of metallic Cu. In addition, no shifts in the BE of Co and Cu peaks are observed indicating the lack of electronic interaction between these atoms. The electronic exchange between Co and B atoms is also not affected by the Cu addition.
4. *Co–Cr–B:* The Cr_{2p} spectrum for Co–Cr–B catalysts exhibits two peaks at 575.7 and 585.3 eV (Fig. 6d), attributed to $Cr_{2p3/2}$ and $2p_{1/2}$ peaks of Cr^{3+} species, respectively. This shows that Cr is in completely oxidized state (Cr_2O_3), which is in agreement

Table 1
Molar ratio (%) of M/(M + Co) (χ_M, where M stands for: Ni, Fe, Cu, Cr, Mo, and W), surface area, maximum H_2 generation rate, ability to act as Lewis acid sites, and activation energy of the as-prepared alloy catalyst powders.

Catalyst powders	M/(M + Co) molar ratio (χ_M)(%)	BET surface area (m^2/g)	Max H_2 generation rate (R_{max}) (ml/min/g catalyst)		Lewis acid	Activation energy (kJ mol^{-1})
			Alkaline $NaBH_4$	Non-alkaline $NaBH_4$		
Co–B	–	20	850	860	No	45
Co–Ni–B	15	22	1175	1160	No	34
Co–Fe–B	35	33	1300	1270	No	31
Co–Cu–B	35	115	2210	2180	No	30
Co–Cr–B	4	40	3400	2250	Yes	37
Co–Mo–B	5	43	2875	2210	Yes	39
Co–W–B	5	54	2570	1940	Yes	41

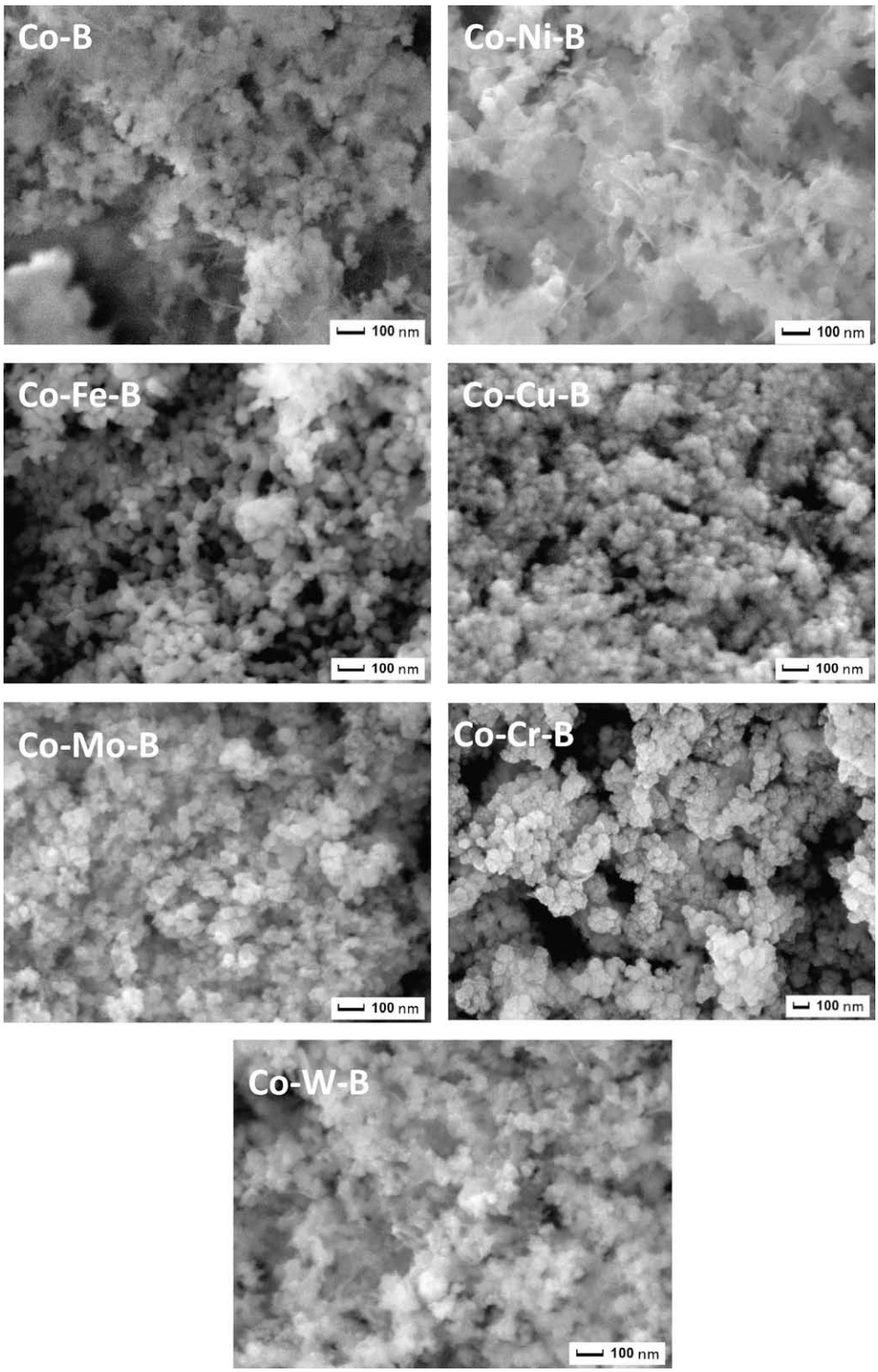

Fig. 3. SEM micrographs of Co–B, Co–Ni–B (χ_{Ni} = 15%), Co–Fe–B (χ_{Fe} = 35%), Co–Cu–B (χ_{Cu} = 35%), Co–Cr–B (χ_{Cr} = 4%), Co–Mo–B (χ_{Mo} = 5%), and Co–W–B (χ_{W} = 5%) powder catalysts.

with the XRD result. It is also noticed that Cr does not modify the electronic interaction between Co and B, because their relevant BEs remain unchanged after the Cr addition.

5. *Co–Mo–B:* The XPS spectra of Mo 3d levels (Fig. 6e) reveal two peaks assigned to MoO_2 (BE of 231.1 and 232.6 eV are ascribed to Mo $3d_{5/2}$ and Mo $3d_{3/2}$ levels of Mo^{4+}, respectively) and two peaks assigned to MoO_3 (BE of 233.7 and 235.8 eV are ascribed to Mo $3d_{5/2}$ and Mo $3d_{3/2}$ levels of Mo^{6+}, respectively). There is no evidence of metallic Mo in the spectra indicating that Mo atoms on the catalyst surface are in completely oxidized state. The BE value for Co and B is unaffected by the addition of Mo in Co–B catalyst.

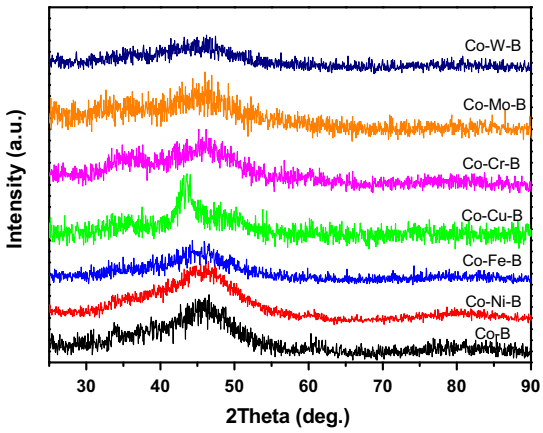

Fig. 4. XRD pattern of Co–B, Co–Ni–B (χ_{Ni} = 15%), Co–Fe–B (χ_{Fe} = 35%), Co–Cu–B (χ_{Cu} = 35%), Co–Cr–B (χ_{Cr} = 4%), Co–Mo–B (χ_{Mo} = 5%), and Co–W–B (χ_{W} = 5%) powder catalysts.

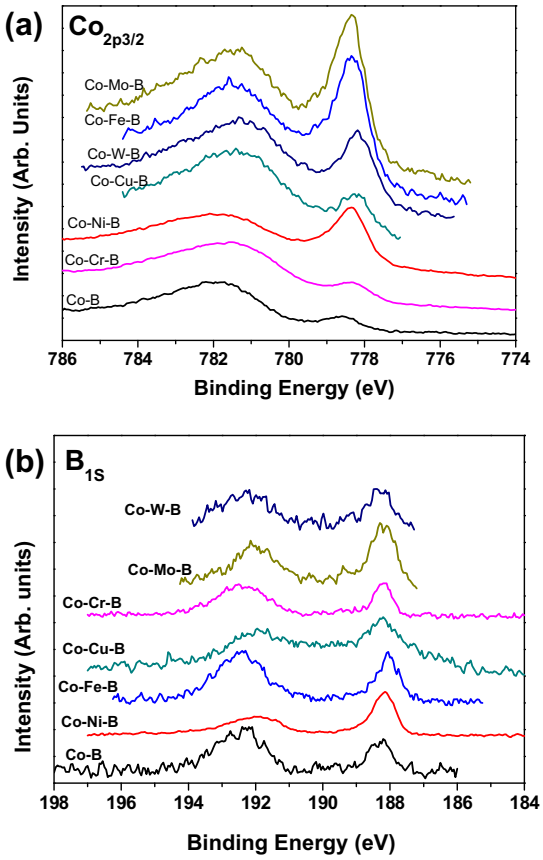

Fig. 5. X-ray photoelectron spectra of $Co_{2p3/2}$ and B_{1s} levels for Co–B, Co–Ni–B (χ_{Ni} = 15%), Co–Fe–B (χ_{Fe} = 35%), Co–Cu–B (χ_{Cu} = 35%), Co–Cr–B (χ_{Cr} = 4%), Co–Mo–B (χ_{Mo} = 5%), and Co–W–B (χ_{W} = 5%) powder catalysts.

6. *Co–W–B:* The W-4f spectrum (Fig. 6f) of Co–W–B catalyst shows the presence of both oxidized and elemental state of W. The XPS spectrum of W $4f_{7/2}$ ($4f_{5/2}$) shows two peaks at BE values of 31.3 (33.4) eV and 35.5 (36.9) eV assigned to metallic W and WO_3 species, respectively. About 33% of the XPS signal rises from elemental W, whereas 67% is associated to the oxidized W. By comparing with the undoped Co–B sample, no significant change in XPS spectra is observed in connection with the presence of the W-dopant: this means that W does not affect the electronic states of Co and B.

The above XPS results prove that all the transition metal dopants in Co–B catalyst exist in different states (elemental, oxidized, oxidized in different proportion). This may be the prime reason to explain the different promoting effects on Co–B catalyst powders as we will discuss in the following sections.

The measured BET surface area of all the catalyst powders is reported in Table 1. The specific surface area decreases in following order: Co–Cu–B > Co–W–B > Co–Mo–B > Co–Cr–B > Co–Fe–B > Co–Ni–B > Co–B. This shows that doping the Co–B catalyst with transition metals (Cr, Mo, W, Fe, Cu, and Ni) causes an increment in the specific surface area irrespective of the type of dopant. However, the trend obtained in the increment of the surface area is quite different from that of the catalytic activity (Fig. 2).

When small amount of Cr, Mo, or W ($\chi_{Cr,Mo,W}$ = 4–5%) is included as a dopant in Co–B, the specific surface area of the catalyst increases by almost 2–2.5 times, a result which is due to the limited particle agglomeration process when compared to pure Co–B (see Fig. 3). Surface characterization (Figs. 3, 5 and 6) of these catalyst powders suggests that Cr, Mo, and W in the form of oxides are located on the surface of the catalyst. These metal oxides act as a kind of atomic barrier between the several Co–B nanoparticles, thus avoiding agglomeration caused by their high surface energy. As a result, the effective surface area increases significantly for Co–Cr–B, Co–Mo–B, and Co–W–B catalyst. A remarkable increment in the surface area, a factor of about 5.5, is observed for Co–Cu–B catalyst when compared to undoped Co–B. As observed by XRD and XPS, the Cu on the catalyst surface is in completely metallic state which prevents the agglomeration of Co–B nanoparticles. The highest surface area of Co–Cu–B is mainly due to the high concentration of Cu when compared to Cr, Mo, and W-dopant in Co–B catalyst. Our previous work proved that when Cr is added at high concentration (χ_{Cr} = 10%) in Co–B catalyst, the surface area increases by one order of magnitude when compared to undoped Co–B catalyst [14]. Similar result is reported by Chen et al. [26] for Mo-promoted Co–B catalyst. However, a deleterious effect in catalytic activity is detected with high concentration of the dopant metals (Cr, Mo, and W) as we will discuss later. Co–Fe–B shows a moderate enhancement in the surface area, when compared to Co–B, even at high concentration of Fe (χ_{Fe} = 35%), probably attributed to the formation of Fe_2O_3 on the surface. On the other hand, negligible rise in surface area is monitored for Co–Ni–B catalyst powder. For the moment, it is not clear why Fe and Ni are ineffective to significantly increase the surface area of Co–B powder.

In a binary metal alloy catalyst, the addition of a new metal, or its oxide, may act as an electrophilic or Lewis acid site for the absorption and activation of the reactants to increase the overall reaction rate. To establish the possible role of the dopant metal as a Lewis acid site in CoB catalyst, it is initially important to recall the $NaBH_4$ hydrolysis mechanism involving a solid-state catalyst. The H_2 production from the metal-catalyzed hydrolysis reaction of $NaBH_4$ takes place, according to Guella et al. [3], by the following kinetics steps: (1) BH_4^- ions are chemisorbed on the metal (Co) atoms; (2) H^- is transferred from BH_4^- to an unoccupied adjacent (Co) metal atom; (3) the hydrogen atom acquires an electron from the metal and leaves the site in hydridic form (H^-), while BH_3^- species remains attached to the Co atom; (4) this H^- reacts with water molecule to produce H_2 and OH^-; and (5) OH^- reacts with boron in BH_3^- to produce the $BH_3(OH)^-$ ion. Again, H^- is transferred from $BH_3(OH)^-$ ion to an unoccupied adjacent (Co) metal atom. The cycle of hydrogen absorption on metal sites continues till $BH_3(OH)^-$ forms $B(OH)_4^-$ and molecular hydrogen is released during each cycle. However, during the last step, the reaction between OH^- and BH_3^- ions is not favored by the catalyst which may cause lower reaction rate. In present Co–B-based alloy catalyst, the dopant metal or its oxides may act as the Lewis acid sites, which are readily

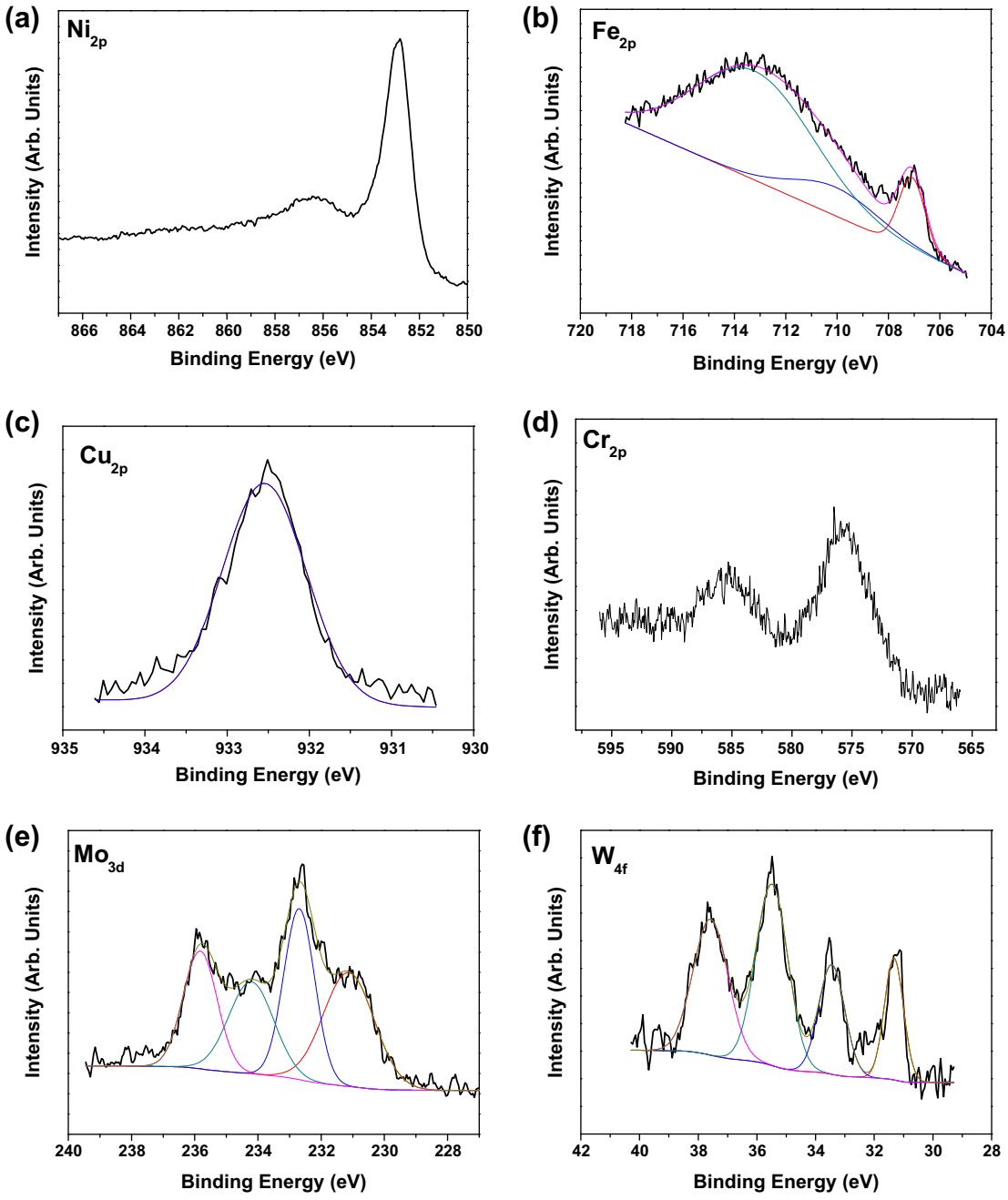

Fig. 6. X-ray photoelectron spectra of (a) Ni_{2p} level for Co–Ni–B (χ_{Ni} = 15%), (b) Fe_{2p} level for Co–Fe–B (χ_{Fe} = 35%), (c) Cu_{2p} level for Co–Cu–B (χ_{Cu} = 35%), (d) Cr_{2p} level for Co–Cr–B (χ_{Cr} = 4%), (e) Mo_{3d} level for Co–Mo–B (χ_{Mo} = 5%), and (f) W_{4f} level for Co–W–B (χ_{W} = 5%) powder catalysts.

available for the absorption of Lewis base such as OH^- ions. During the hydrolysis reaction, the hydroxyl molecule in the solution can be absorbed on these sites via donating the lone electron from OH^- group. This bonding polarizes the hydroxyl group, which creates favorable condition for the reaction with BH_3^- ions attached to the neighboring active Co sites and thus increasing the overall reaction rate.

A set of experiments was conducted to find out which dopant transition metal in Co–B catalyst acts as Lewis acid site to assist the absorption of the OH^- ions. For the catalytic hydrolysis reaction, two types of hydride solution (0.025 M) were prepared, namely: (1) $NaBH_4$ solution stabilized with NaOH (0.025 M) (designated as solution A) and (2) $NaBH_4$ solution without NaOH (designated as solution B). The hydrogen generation rate was measured by hydrolysis of solutions A and B using all the alloy catalyst powders and reported in Table 1. No significant change in H_2 generation rate was observed through hydrolysis of alkaline and non-alkaline $NaBH_4$ in the presence of Co–B, Co–Ni–B, Co–Fe–B, or Co–Cu–B catalyst powders. On the contrary, the H_2 generation rate obtained in the presence of Co–Cr–B, Co–Mo–B, or Co–W–B for solution A was much higher than that of solution B. This proves that during the hydrolysis reaction, in the presence of hydroxyl molecule in the solution, Cr, Mo, and W species, in the form of oxides, act as the Lewis acid sites to absorb the OH^- group and catalyze the reaction between OH^- and boron species (BH_3^-, $BH_2(OH)^-$, and $BH(OH)_2^-$). However, it is observed that the increment in H_2 generation rate, by addition of NaOH during the hydrolysis of $NaBH_4$, is far better for Co–Cr–B catalyst when compared to

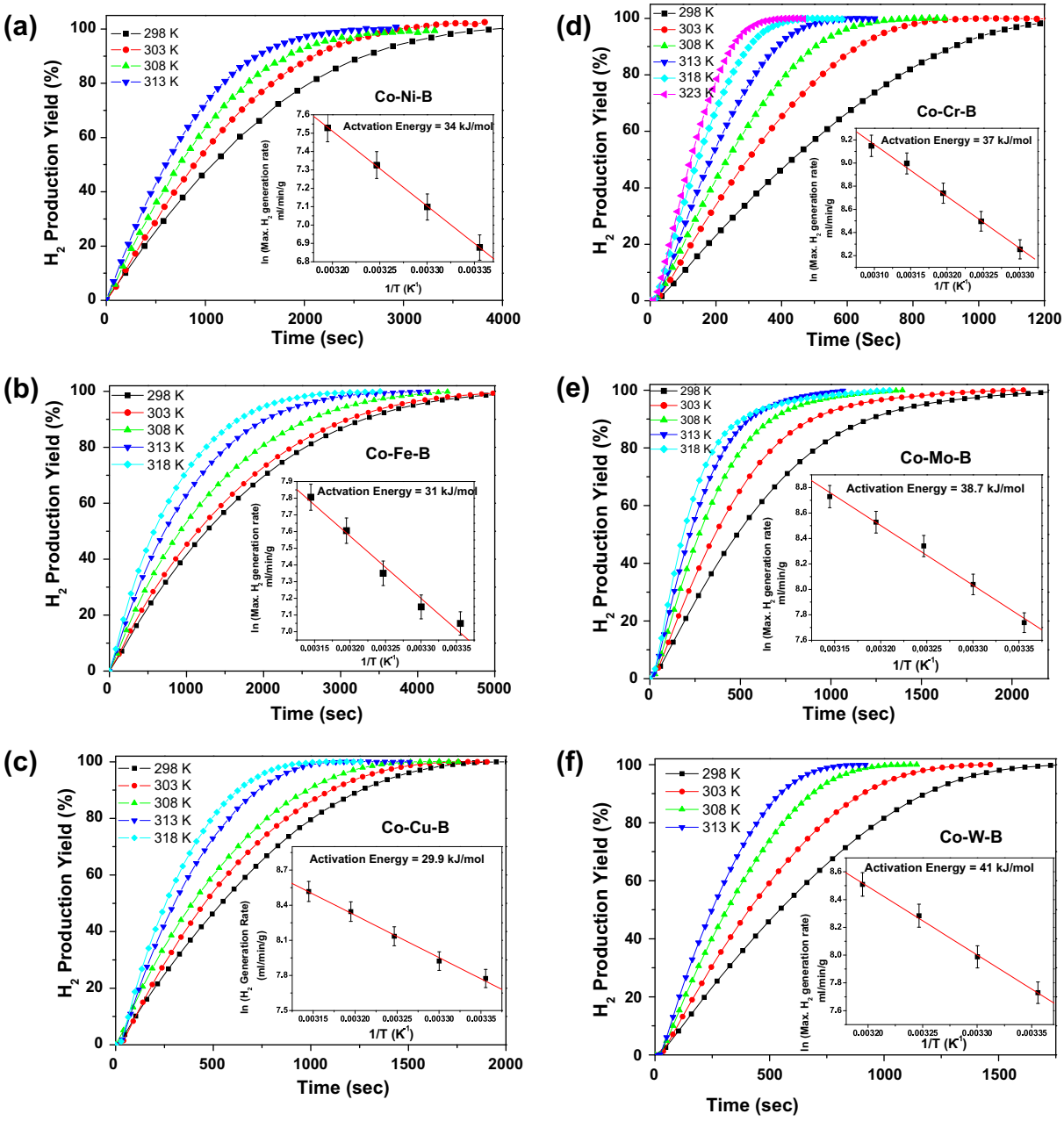

Fig. 7. Hydrogen generation yield as a function of reaction time by hydrolysis of alkaline $NaBH_4$ (0.025 M) solution measured at different solution temperatures with (a) Co–Ni–B (χ_{Ni} = 15%), (b) Co–Fe–B (χ_{Fe} = 35%), (c) Co–Cu–B (χ_{Cu} = 35%), (d) Co–Cr–B (χ_{Cr} = 4%), (e) Co–Mo–B (χ_{Mo} = 5%), and (f) Co–W–B (χ_{W} = 5%) powder catalysts. Inset shows the Arrhenius plot of the H_2 generation rates.

Co–Mo–B or Co–W–B catalyst powders. The Cr^{3+} species might have a stronger affinity for the oxygen of hydroxyl group than W^{4+} or Mo^{4+} species, thus Cr-additives exhibit a stronger promoting effect than Mo- or W-additives.

The role of each dopant transition metal in Co–B catalyst, in enhancing the H_2 generation rate, is now underlined on the basis of the characterization results of the alloy powder catalysts.

1. *Co–Ni–B catalyst:* Nickel on the catalyst surface is mostly in a metallic state, which neither increases significantly the surface area of Co–B powder nor acts as a Lewis acid site for OH^- ions absorption. However, Ni is able to increase the density of electrons on the Co active sites due to boron enrichment. These electron-enriched metal active sites will favor the catalysis reaction by providing the electrons required by the hydrogen atom during the hydrolysis reaction. Thus, the catalytic activity is moderately higher for Co–Ni–B catalyst, when compared to the Co–B, due to the electron-enriched active metal site: this is the case for the Ni-doping concentration with χ_{Ni} = 10% and 15%. However, the H_2 generation rate is maximum with χ_{Ni} = 15% and further increase in Ni concentration causes the activity to decrease. As observed in our previous work [16], Co–B shows much higher catalytic activity when compared to Ni–B for hydrolysis of $NaBH_4$, thus indicating that Co metal is a more active site than Ni for catalytic hydrolysis reaction. The decrement in the activity by increasing the amount in Ni is due to the fact that more active Co sites are replaced by less active Ni sites.

2. *Co–Fe–B catalyst:* By increasing χ_{Fe}, the activity of Co–Fe–B catalyst first increases and then decreases. The maximum activity is obtained with χ_{Fe} = 35%. By knowing that Fe–B alloy catalyst is less active than Co–B for the hydrolysis of $NaBH_4$, it is easily understood that only metallic Co acts as a main active site in the Co–Fe–B alloy and that Fe-dopant behaves as a promoter. At χ_{Fe} values from 10% to 35%, the promoting effect of Fe-dopant is mainly attributed to the increased surface area of the Co–Fe–B catalyst due to the existence of Fe_2O_3 species, on the catalyst surface, which act as an inhibitor against agglomeration of the Co–B particles. The presence of a little amount of metallic Fe could also make a minor contribution to the enhancement of catalytic activity by electron transfer to the active Co sites as observed by XPS (Fig. 6b). Electron-enriched Co active sites will facilitate the catalysis reaction as explained for previous Co–Ni–B catalyst. At larger concentration of Fe-dopant, the catalytic activity decreases because too many surface Co active sites would be covered by inactive Fe species.
3. *Co–Cu–B catalyst:* As with the above two catalysts, Co–Cu–B catalyst also requires high dopant (Cu) concentration to have the promoting effect. The catalytic activity increases with the amount of Cu-dopant in Co–B alloy catalyst, it reaches maximum at the optimum concentration of χ_{Cu} = 35%, then it decreases. Copper, in fully metallic state, is unable to either cause any electron transfer to active Co site or act as Lewis acid site for OH^- ions absorption. However, Cu on the catalyst surface acts as a promoter by increasing the specific surface area by more than five times, when compared to Co–B catalyst, by preventing particle agglomeration. According to the above reported hydrolysis reaction mechanism [3], the initial reaction occurs between BH_4^- ions and metal sites, which means that the reaction rate is proportional to the number of available metal sites for the absorption of BH_4^- ions in the solution. In this reaction scheme, the Co–Cu–B catalyst powder, having a surface area almost five times higher than that of Co–B, may provide an ideal condition for BH_4^- ions absorption for catalytic hydrolysis reaction. However, a concentration of the Cu promoters exceeding χ_{Cu} = 35% is deleterious to the hydrolysis reaction, because major portion of the surface Co active sites would be covered by the Cu metallic species.
4. *Co–Cr–B, Co–Mo–B, and Co–W–B catalysts:* These three powders seem to be acting as a catalyst with a similar mechanism, because in all the three cases, a small amount of dopant (Cr, Mo, or W) is enough to create the promoting effect in the Co–B catalyst. Even in these cases, by increasing the dopant concentration, the activity first increases and then decreases. The optimum contents of Cr-, Mo-, and W-promoters are: χ_{Cr} = 4%, χ_{Mo} = 5%, and χ_W = 5%, respectively. The promoting effect is mainly caused by the corresponding oxide species of the dopant transition metals (Cr, Mo, or W) which, on the catalyst surface, inhibit the particle agglomeration thus increasing the surface area of the Co–B catalyst by favoring a better dispersion of the particles. In addition, the Cr^{3+}, Mo^{4+}, and W^{4+} species also act as Lewis acid sites for OH^- absorption due to the strong affinity of these sites toward oxygen of the OH^- group. A polarization of the O–H bond occurs which favors the reaction between hydroxyl group and boron species attached to the neighboring Co active sites. In conclusion, the oxide species provide high surface area and act as Lewis absorption sites for OH^- ions: these are the two main reasons involved in the significant enhancement of R_{max} observed for Co–Cr–B, Co–Mo–B, and Co–W–B catalysts with respect to that observed with the Co–B catalyst. Cr-doped Co–B shows the highest R_{max} when compared to W- and Mo-doping: this is attributed to the superior capability of Cr^{3+} species to absorb OH^- group ions. The deleterious effect on catalytic activity at higher dopant content is attributed to the surface covering of the active Co metal by Cr, Mo, or W species.

To summarize, the transition metals Ni, Fe, Cu, Cr, Mo, and W, when added to the Co–B, promote the catalysis efficiency through three effects, namely by:

1. Creating higher electron density on to the active Co sites.
2. Increasing the specific surface area of the final catalyst powder by inhibiting Co–B particle agglomeration and thus favouring better particle dispersion.
3. Acting, in the form of oxides on the catalyst surface, as the Lewis acid sites for the absorption of OH^- group ions and catalyzing its reaction with boron species.

The investigated transition metals are able to enhance the catalytic efficiency of the Co–B catalyst by only one of the three above effects (Co–Ni–B and Co–Cu–B catalyst) or a combination of two effects (Co–Cr–B, Co–Mo–B, Co–W–B, and Co–Fe–B catalyst).

To conclude the analysis of the doped Co–B catalysts, the H_2 generation yield as a function of time was measured at different solution temperatures by hydrolysis of alkaline $NaBH_4$ (0.025 M) solution using Co–Ni–B (χ_{Ni} = 15%), Co–Fe–B (χ_{Fe} = 35%), Co–Cu–B (χ_{Cu} = 35%), Co–Cr–B (χ_{Cr} = 4%), Co–Mo–B (χ_{Mo} = 5%), and Co–W–B (χ_W = 5%) powder catalysts as reported in Fig. 7a–f, respectively. As expected, H_2 generation rate increases with the temperature. Using the Arrhenius plot (inset of Fig. 7) for the hydrogen production rate, the activation energies are obtained and summarized in Table 1. The results clearly show that in Co–B catalyst doped with transition metal, the activation energy is always lower when compared to undoped Co–B catalyst powder (45 kJ mol^{-1}) [16]. In general, the obtained activation energies are lower than that obtained with Raney Co (53.7 kJ mol^{-1}) [6], carbon supported Co–B (57.8 kJ mol^{-1}) and Co–B nanoparticles (42.7 kJ mol^{-1}) [27]. The values are also lower than that found by Amendola (47 kJ mol^{-1}) [4] by using Ru catalyst. Kaufman and Sen [28], by using different bulk metal catalysts, obtained 75 kJ mol^{-1} for cobalt, 71 kJ mol^{-1} for nickel, and 63 kJ mol^{-1} for Raney nickel. The activation energy values obtained in the present case are comparable to that obtained with nanoparticle-assembled Co–B thin film (30 kJ mol^{-1}) [12], Pd/C powder (28 kJ mol^{-1}) [29], Co supported on γ-Al_2O_3 (33 kJ mol^{-1}) [9], Ru nanoclusters (29 kJ mol^{-1}) [5], and Ru-C (37 kJ mol^{-1}) [30]. The favorable activation energy values obtained in the present work are attributed to promoting effects, caused by the different transition metals, to enhance the catalytic hydrolysis reaction.

4. Conclusions

We have investigated the role of the dopant transition metals: Ni, Fe, Cu, Cr, Mo, and W on the catalytic efficiency of the Co–B powder for H_2 generation by hydrolysis of $NaBH_4$. Transition metals added to the Co–B catalyst behave in a different way while influencing the catalytic activity. Cr, W, Mo, and Cu impose significant catalytic effects by increasing 3–4 times the H_2 generation rate when compared to the Co–B catalyst. On the contrary, Ni and Fe cause only marginal increment in the catalytic performance of the Co–B catalyst. The metal/(Co + metal) molar ratio was varied in order to study the effect of each metal dopant concentration on the catalytic efficiency. We observed that the best promoting effects are obtained with specific molar concentration of the transition metals. The promoting effects of the dopants are related to: (1) large active surface area of the catalysts (Co–Fe–B, Co–Cu–B, Co–Cr–B, Co–Mo–B, Co–W–B), (2) ability to act as Lewis acid sites for better absorption of OH^- groups (Co–Cr–B, Co–Mo–B, Co–W–B),

(3) electronic interaction with Co active metal (Co–Ni–B, Co–Fe–B), and (4) amorphous nature of the alloy catalyst (all investigated catalysts). Finally, all the activation energies involved in the catalytic hydrolysis of $NaBH_4$ are comparable to the lowest values of the reported literature catalysts.

Acknowledgements

We thank N. Bazzanella for SEM–EDS analysis, C. Armellini for XRD analysis, S. Dirè for BET measurements, and S. Torrengo for XPS analysis. The research activity is financially supported by the Hydrogen-FISR Italian project.

References

[1] S.C. Amendola, S.L. Sharp-Goldman, M.S. Janjua, M.T. Kelly, P.J. Petillo, M. Binder, J. Power Sour. 85 (2000) 186.
[2] Jaeyoung lee, Kyung Yong Kong, Chang Ryul Jung, Eunae Cho, Sung Pil Yoon, Jonghee Han, Tai-Gyu Lee, Suk Woo Nam, Catal. Today 120 (2007) 305.
[3] G. Guella, C. Zanchetta, B. Patton, A. Miotello, J. Phys. Chem. B 110 (2006) 17024.
[4] S.C. Amendola, S.L. Sharp-Goldman, M.S. Janjua, N.C. Spencer, M.T. Kelly, P.J. Petillo, M. Binder, Int. J. Hydrogen Energy 25 (2000) 969.
[5] S. Özkar, M. Zahmakiran, J. Alloys Compd. 404–406 (2005) 728.
[6] B.H. Liu, Z.P. Li, S. Suda, J. Alloys Compd. 415 (2006) 288.
[7] N. Patel, G. Guella, A. Kale, A. Miotello, B. Patton, C. Zanchetta, L. Mirenghi, P. Rotolo, Appl. Catal. A: Gen. 323 (2007) 18.
[8] Y. Pei, P. Guo, M. Qiao, H. Li, S. Wei, H. He, K. Fan, J. Catal. 248 (2007) 303.
[9] W. Ye, H. Zhang, D. Xu, L. Ma, B. Yi, J. Power Sour. 164 (2007) 544.
[10] P. Krishnan, S. Advani, A.K. Prasad, Appl. Catal. B 86 (2009) 137.
[11] Dong-ge Tong, Wei Chu, Yong-yue Luo, Hong Chen, Xiao-yang Ji, J. Mol. Catal. A: Chem. 269 (2007) 149.
[12] N. Patel, R. Fernandes, G. Guella, A. Kale, A. Miotello, B. Patton, C. Zanchetta, J. Phys. Chem. C 112 (2008) 6968.
[13] H. Li, J.F. Deng, J. Chem. Technol. Biotechnol. 76 (2001) 985.
[14] R. Fernandes, N. Patel, A. Miotello, Appl. Catal. B: Environ. 92 (2009) 68.
[15] J. Fang, X. Chen, B. Liu, S. Yan, M. Qiao, H. Li, H. He, K. Fan, J. Catal. 229 (2005) 97.
[16] R. Fernandes, N. Patel, A. Miotello, M. Filippi, J. Mol. Catal. A: Chem. 298 (2009) 1.
[17] N. Patel, R. Fernandes, A. Miotello, J. Power Sour. 188 (2009) 411.
[18] R. Fernandes, N. Patel, A. Miotello, Int. J. Hydrogen Energy 34 (2009) 2893.
[19] D.A. Lyttle, E.H. Jensen, W.A. Struck, Anal. Chem. 24 (1952) 1843.
[20] C. Zanchetta, B. Patton, G. Guella, A. Miotello, Meas. Sci. Technol. 18 (2007) N21.
[21] A. Baiker, Faraday Discuss. Chem. Soc. 87 (1989) 239.
[22] W.L. Dai, M.H. Qiao, J.F. Deng, Appl. Surf. Sci. 120 (1997) 119.
[23] B.H. Liu, Q. Li, Int. J. Hydrogen Energy 33 (2009) 7385.
[24] H. Li, W. Wang, H. Li, J.F. Deng, J. Catal. 194 (2000) 211.
[25] H. Li, Y. Wu, J. Zhang, W. Dai, M. Qiao, Appl. Catal. A: Gen. 275 (2004) 199.
[26] X. Chen, H. Li, H. Luo, M. Qiao, Appl. Catal. A: Gen. 233 (2002) 13.
[27] A. Garron, D. Swierczynski, S. Bennici, A. Auroux, Int. J. Hydrogen Energy 34 (2009) 1185.
[28] C.M. Kaufman, B. Sen, J. Chem. Soc., Dalton Trans. 2 (1985) 307.
[29] N. Patel, B. Patton, C. Zanchetta, R. Fernandes, G. Guella, A. Kale, A. Miotello, Int. J. Hydrogen Energy 33 (2008) 287.
[30] Y. Shang, R. Chen, Energy Fuels 20 (2006) 2149.